(12) **United States Patent**
Eom et al.

(10) **Patent No.:** **US 9,627,490 B1**
(45) **Date of Patent:** **Apr. 18, 2017**

(54) **EPITAXIAL GROWTH OF HIGH QUALITY VANADIUM DIOXIDE FILMS WITH TEMPLATE ENGINEERING**

(71) Applicant: **Wisconsin Alumni Research Foundation**, Madison, WI (US)

(72) Inventors: **Chang-Beom Eom**, Madison, WI (US); **Daesu Lee**, Madison, WI (US)

(*) Notice: Subject to any disclaimer, the term of this patent is extended or adjusted under 35 U.S.C. 154(b) by 0 days.

(21) Appl. No.: **14/974,178**

(22) Filed: **Dec. 18, 2015**

(51) **Int. Cl.**

H01L 29/24	(2006.01)
H01L 21/02	(2006.01)
H01L 21/36	(2006.01)
H03K 17/56	(2006.01)
H01L 29/78	(2006.01)
H01L 29/66	(2006.01)
H01L 29/10	(2006.01)
H03K 17/687	(2006.01)
H01L 45/00	(2006.01)
H03K 17/51	(2006.01)

(52) **U.S. Cl.**
CPC *H01L 29/24* (2013.01); *H01L 21/02414* (2013.01); *H01L 21/02483* (2013.01); *H01L 21/02565* (2013.01); *H01L 29/1033* (2013.01); *H01L 29/1079* (2013.01); *H01L 29/66969* (2013.01); *H01L 29/78* (2013.01); *H01L 45/1206* (2013.01); *H01L 45/146* (2013.01); *H03K 17/51* (2013.01); *H03K 17/687* (2013.01)

(58) **Field of Classification Search**
CPC H01L 29/24; H01L 29/78; H01L 29/1033; H01L 29/1079; H01L 29/66969; H01L 21/02414; H01L 21/02483; H01L 21/02565; H01L 45/146; H01L 45/1206; H03K 17/687; H03K 17/51
USPC 257/3, 43, 108, 295, 421, E21.009, 257/E21.021, E21.461, E27.104, E29.1; 327/365; 365/145; 204/192.11, 192.15, 204/192.34; 438/99, 104, 381
See application file for complete search history.

(56) **References Cited**

U.S. PATENT DOCUMENTS

3,547,594 A	12/1970	Teeg
6,653,704 B1	11/2003	Gurney
7,583,176 B1	9/2009	Robinson
8,864,957 B2	10/2014	Ramanathan
8,871,363 B2	10/2014	Tsuchiya
2008/0032441 A1*	2/2008	Hirai H01L 51/00 438/99
2009/0213636 A1*	8/2009	Koinuma B01J 23/002 365/145

(Continued)

OTHER PUBLICATIONS

A. Atrei et al., Composition and structure of ultrathin vanadium oxide layers deposited on SnO2(110), Surface Science 513, 2002, pp. 149-162.
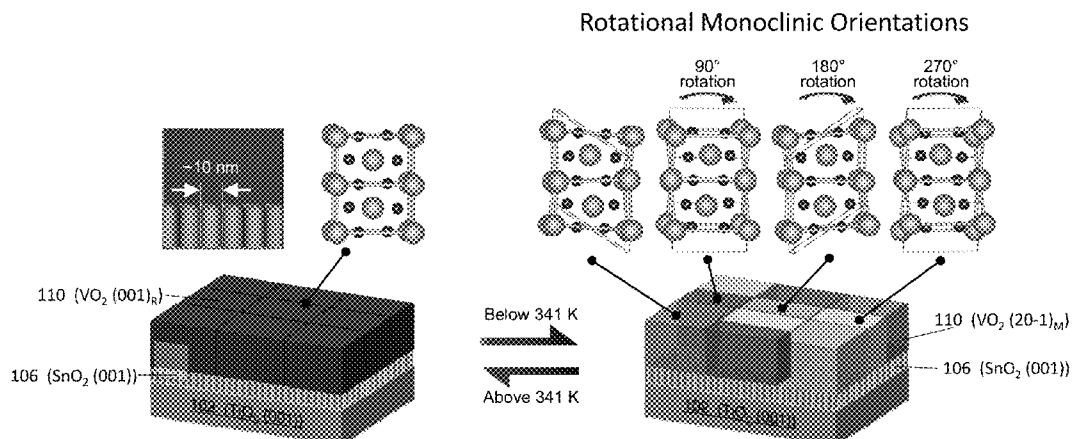
(Continued)

Primary Examiner — Dao H Nguyen
(74) *Attorney, Agent, or Firm* — Bell & Manning, LLC

(57) **ABSTRACT**

Layered oxide structures comprising an overlayer of high quality VO_2 and methods of fabricating the layered oxide structures are provided. Also provided are high-speed switches comprising the layered structures and methods of operating the high-speed switches. The layered oxide structures include high quality VO_2 epitaxial films on isostructural SnO_2 growth templates.

15 Claims, 12 Drawing Sheets

Rotational Monoclinic Orientations

90° rotation   180° rotation   270° rotation

110 $\{VO_2 (001)_R\}$
106 $\{SnO_2 (001)\}$

Below 341 K
Above 341 K

110 $\{VO_2 (20-1)_M\}$
106 $\{SnO_2 (001)\}$

(56) **References Cited**

U.S. PATENT DOCUMENTS

2010/0314617 A1*	12/2010	Ito	B81C 1/00111
			257/43
2011/0151639 A1*	6/2011	Lim	C01G 23/047
			438/381
2011/0175047 A1*	7/2011	Ramanathan	H01L 49/003
			257/2
2011/0181345 A1*	7/2011	Ramanathan	G11C 11/16
			327/509
2014/0266391 A1*	9/2014	Parkin	H01L 45/04
			327/365
2015/0340607 A1*	11/2015	Ramanathan	G11C 11/16
			438/104

OTHER PUBLICATIONS

Hyun Koo et al., Effect of Oxide Buffer Layer on the Thermochromic Properties of VO2 Thin Films, Journal of Materials Engineering and Performance, vol. 22 (12), Oct. 1, 2013, pp. 3967-3972.

R. Molaei et al., A microstructural approach toward the effect of thickness on semiconductor-to-metal transition characteristics of VO2 epilayers, Journal of Applied Physics 115, 164311, Apr. 29, 2014, pp. 1-8.

Zongtao Zhang et al., Solution-based fabrication of vanadium dioxide on F:SnO2 substrates with largely enhanced thermochromism and low-emissivity for energy-saving applications, Energy & Environmental Science, DOI: 10.1039/c1ee02092g, Sep. 8, 2011, pp. 1-8.

Matthias Batzill et al., The surface and materials science of tin oxide, Progress in Surface Science 79, 2005, pp. 47-154.

O.M. Osmolovskaya et al., Synthesis of Vanadium Dioxide Thin Films and Nanopowders: A Brief Review, Rev. Adv. Mater. Sci. 38, 2014, pp. 70-74.

Tsung-Han Yang et al., On growth of epitaxial vanadium oxide thin film on sapphire (0001), Journal of Materials Research, vol. 25, Issue 03 , Mar. 2010, pp. 422-426.

Feliks Chudnovskiy et al., Switching device based on first-order metal insulator transition induced by external electric field, Future Trends in Microelectronics: the Nano Millennium, 2002, pp. 148-155.

Gisia Beydaghyan et al., High contrast thermochromic switching in vanadium dioxide (VO2) thin films deposited on indium tin oxide substrates, Thin Solid Films 522, Jul. 28, 2012, pp. 204-207.

A. Atrei et al., XPD Study of Vanadium Oxide Films Grown on the SnO2(110) Surface, Surface Review and Letters, vol. 6, No. 6, 1999, pp. 1187-1193.

You Zhou et al., Voltage-triggered Ultra-fast Metal-insulator Transition in Vanadium Dioxide Switches, IEEE Electron Device Letters, 34, 202, 2013, pp. 1-7.

Yaoming Sun et al., Anisotropic vanadium dioxide sculptured thin films with superior thermochromic properties, Scientific Reports 3:2756, Sep. 25, 2013, pp. 1-10.

Mikhail Esaulkov et al., Emission of terahertz pulses from vanadium dioxide films undergoing metal-insulator phase transition, Optica vol. 2, No. 9, Sep. 4, 2015, pp. 790-796.

Zheng Yang et al., Oxide Electronics Utilizing Ultrafast Metal-Insulator Transitions, Annu. Rev. Mater Res. 41, Mar. 30, 2011, pp. 337-367.
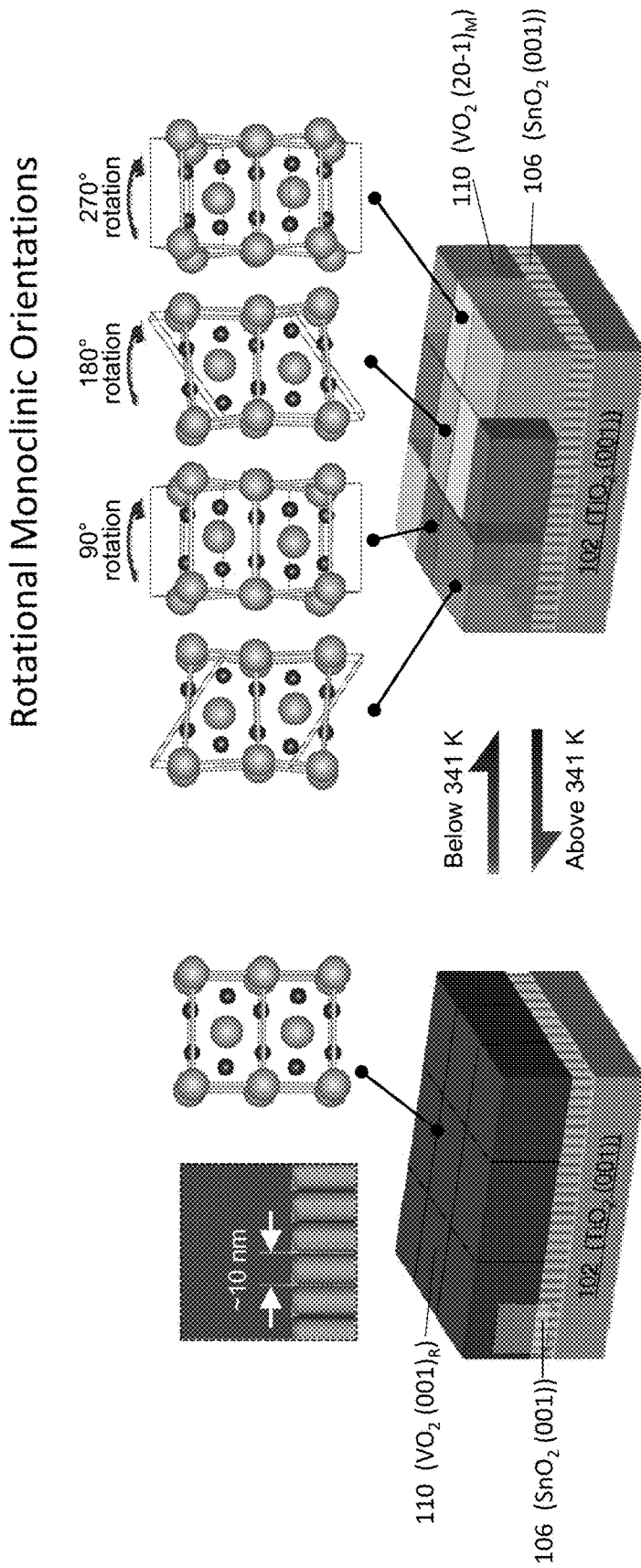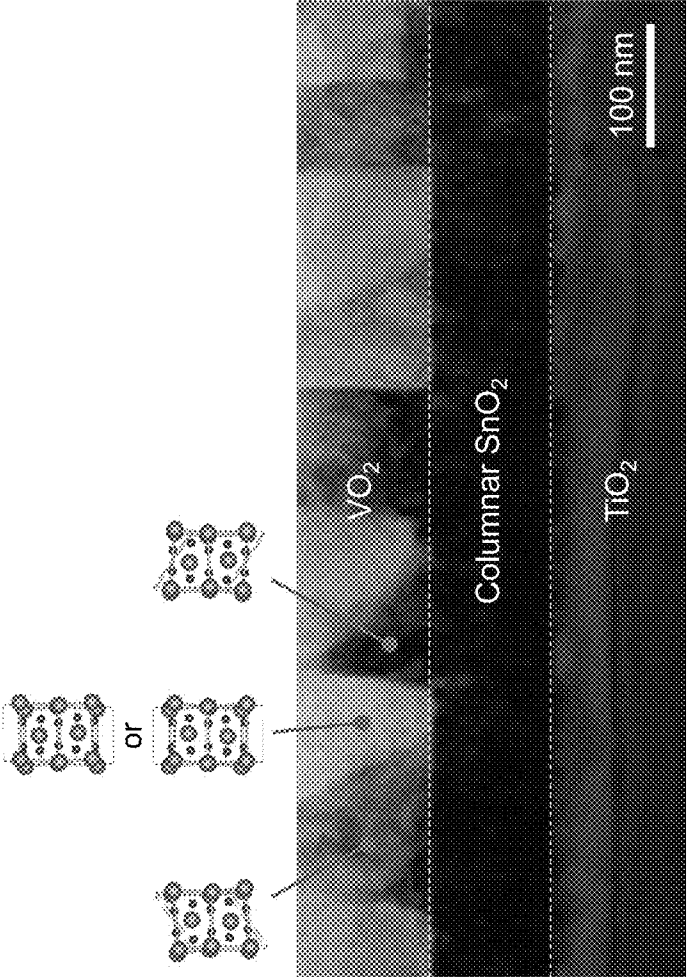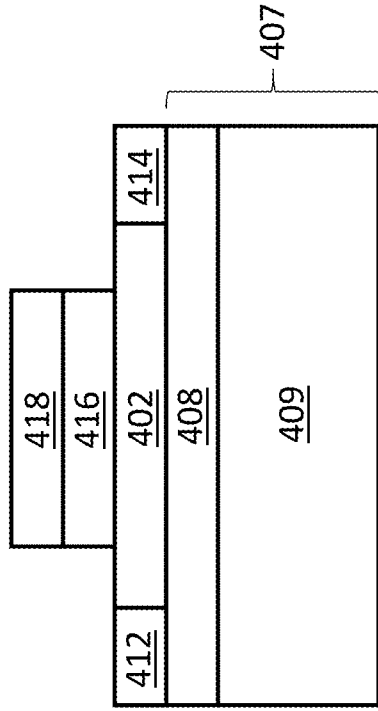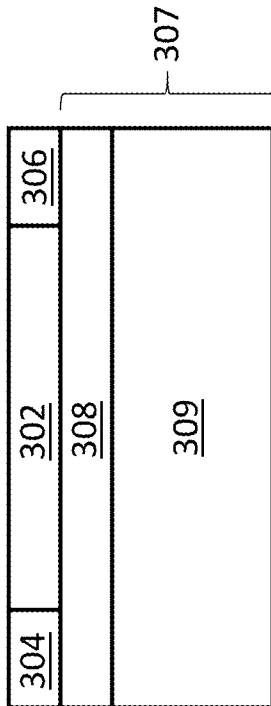
* cited by examiner

FIG. 1

FIG. 2

FIG. 4

FIG. 3

FIG. 5A

VO₂ rutile metal

2.87 Å   4.55 Å

c_R b_R a_R

Monoclinic insulator

~2.89 Å   ~4.52 Å

a_M b_M c_M

FIG. 5B

$\Delta a/a_{bulk} \approx 1\%$

VO₂   TiO₂

Strain   High   O

FIG. 5C

4%   3%

VO₂   SnO₂   TiO₂
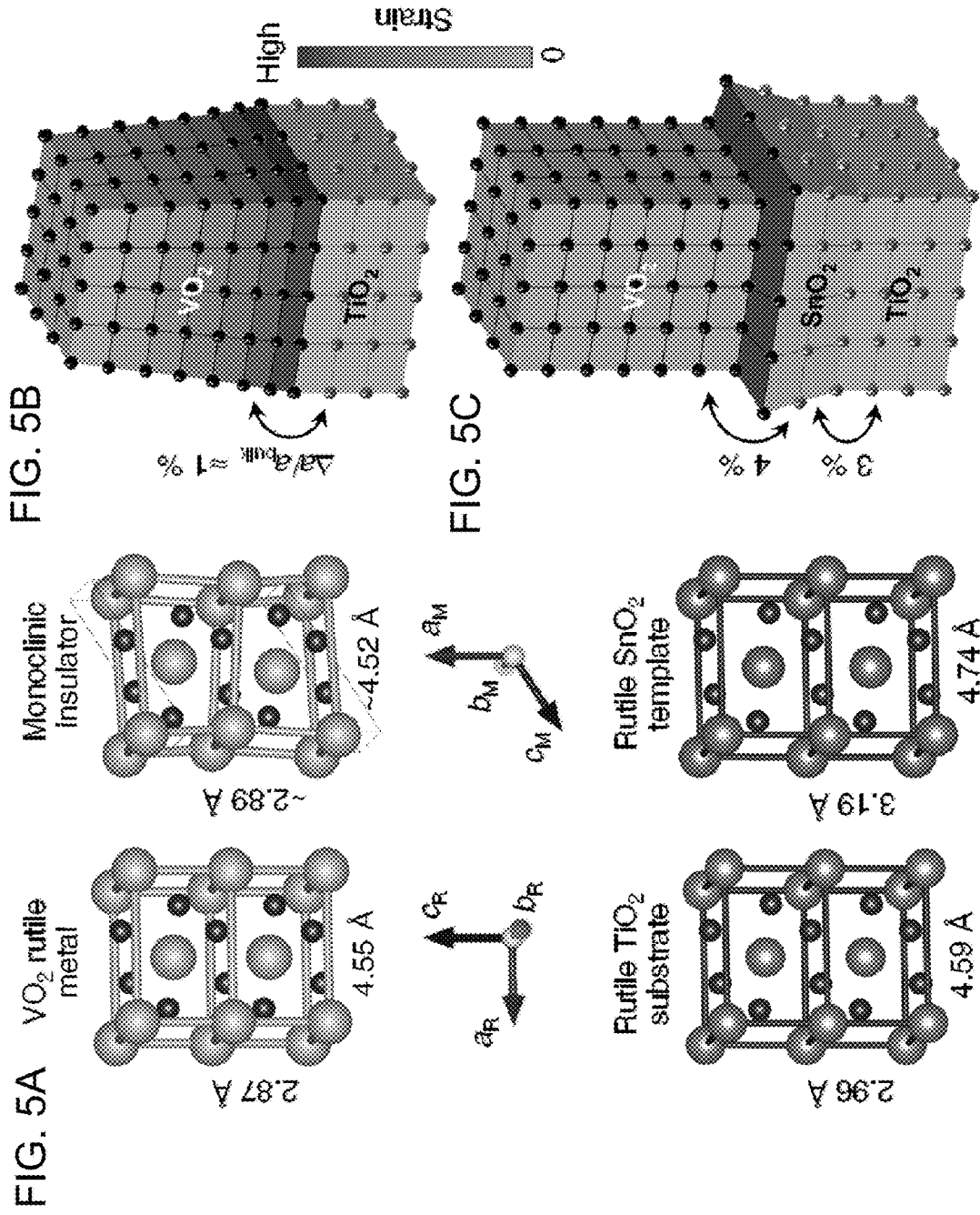
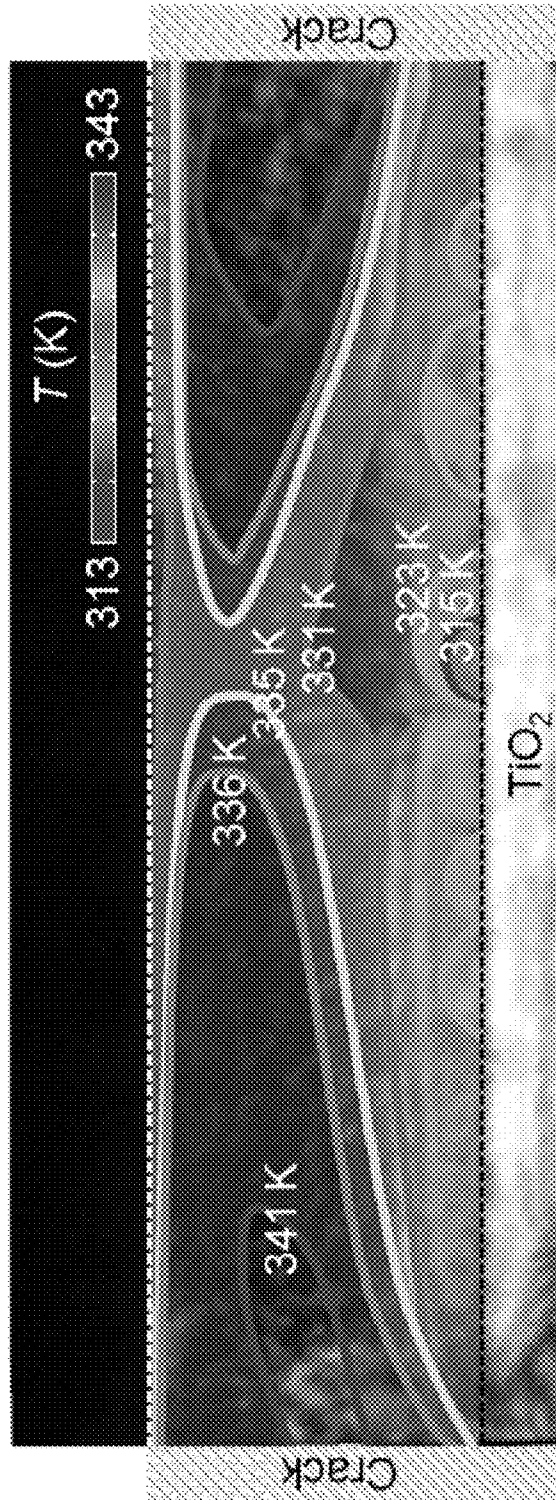Rutile SnO₂ template

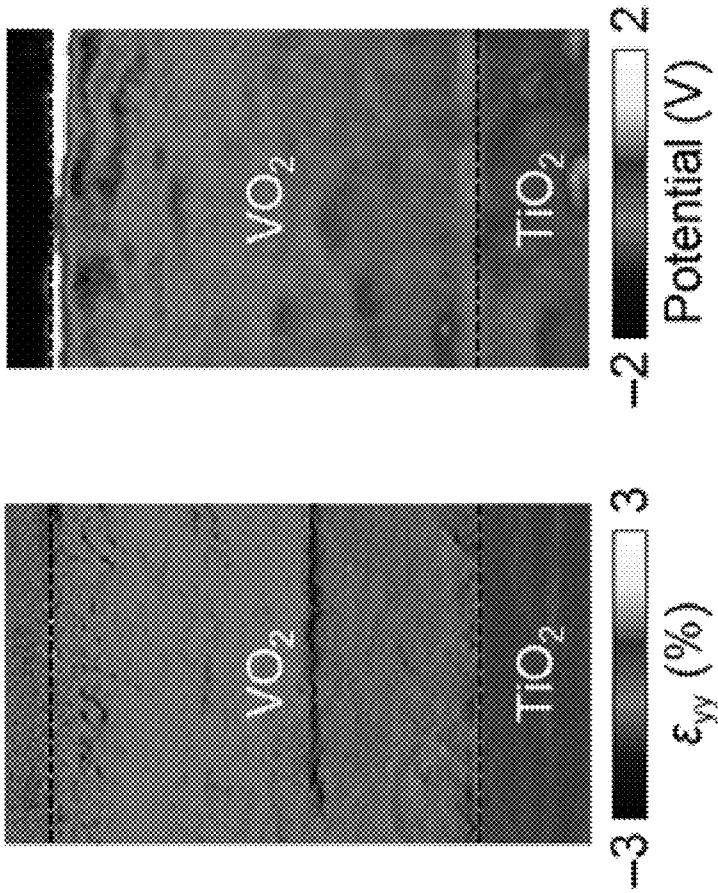3.19 Å   4.74 Å

Rutile TiO₂ substrate

2.96 Å   4.59 Å

FIG. 6A

FIG. 6C

FIG. 6B
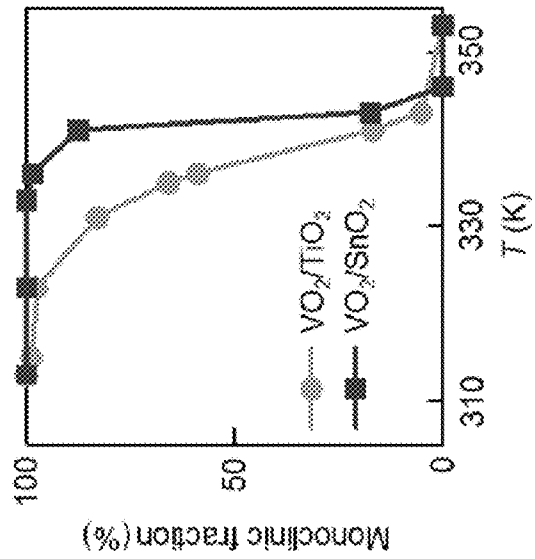
FIG. 6E

FIG. 6D

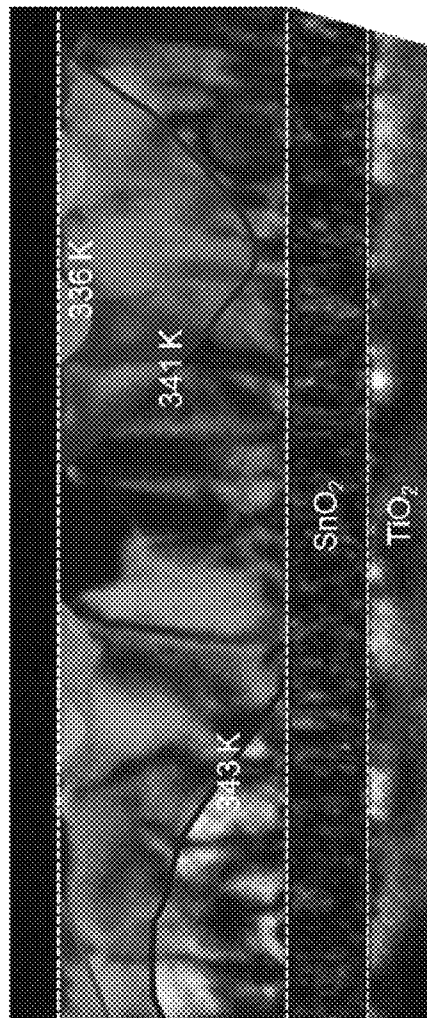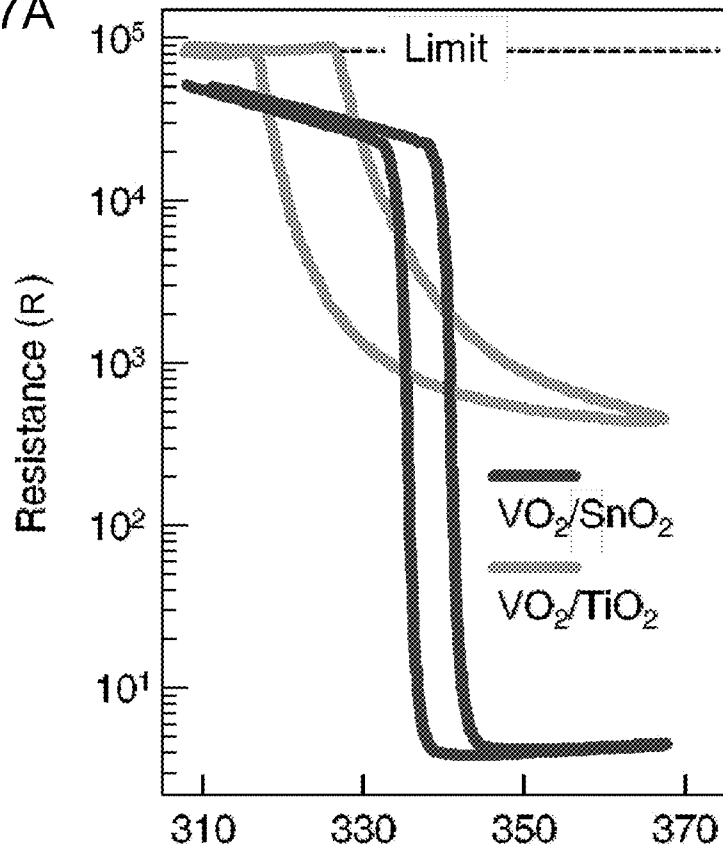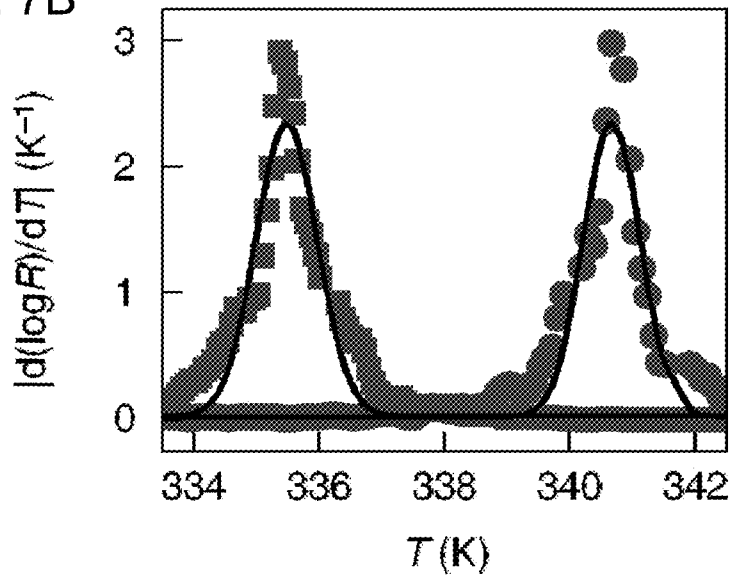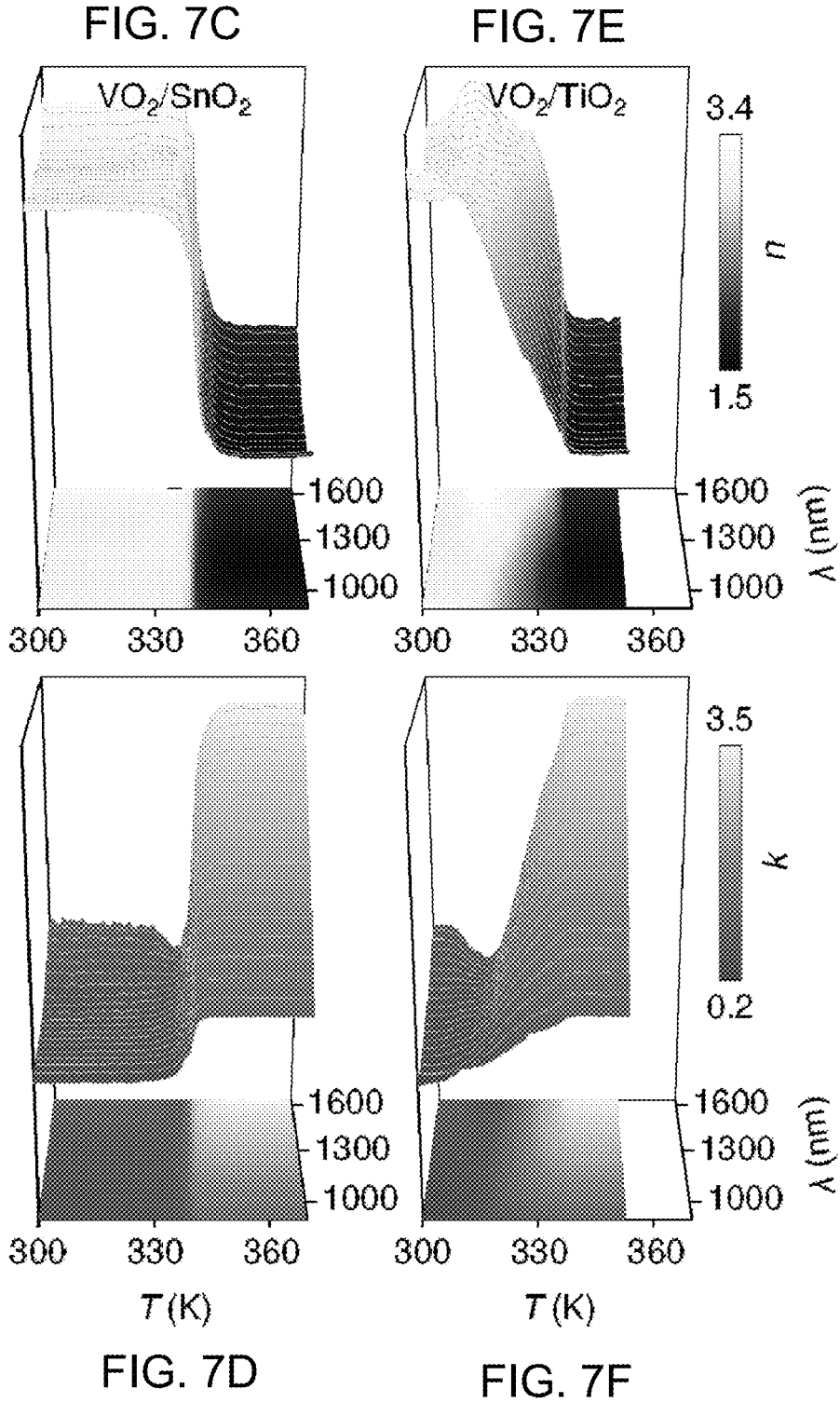FIG. 7A

FIG. 7B

FIG. 7C

FIG. 7E

FIG. 7D

FIG. 7F
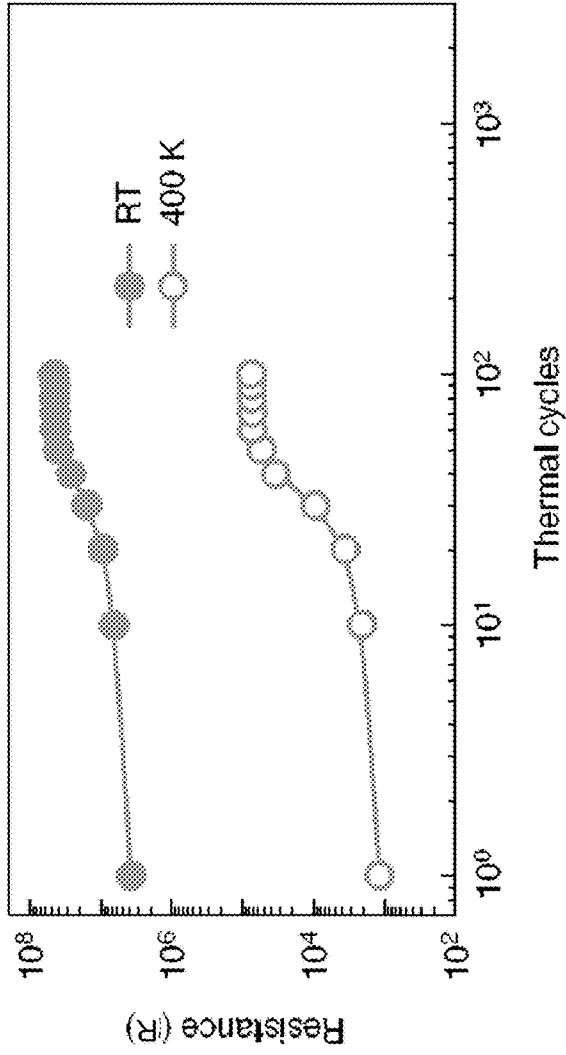
FIG. 8B

FIG. 8A

FIG. 8D

FIG. 8C

FIG. 9A

FIG. 9B

EPITAXIAL GROWTH OF HIGH QUALITY VANADIUM DIOXIDE FILMS WITH TEMPLATE ENGINEERING

REFERENCE TO GOVERNMENT RIGHTS

This invention was made with government support under N00014-13-1-0183 awarded by the United States Navy. The government has certain rights in the invention.

BACKGROUND

VO_2 is a fascinating correlated-oxide material that possesses strong coupling among its charge, spin, orbital, and lattice degrees of freedom. VO_2 exhibits a sharp metal-insulator transition (MIT) above room temperature (i.e., transition temperature T_{MIT} of ~341 K in bulk) with an accompanying structural-phase transition from high-temperature rutile to low-temperature monoclinic structures. This unique property coupled with an almost five-orders-of-magnitude conductivity change (in single-crystal bulks) across the transition make VO_2 a compelling model system for scientific and technological endeavors. Furthermore, the ultrafast nature of VO_2's MIT gives it diverse potential applications in materials physics and solid-state electronics. Critical to any practical application for VO_2, as well as to exploration of its fundamental physics, is the ability to grow high-quality epitaxial thin films.

Yet it has been difficult to achieve heteroepitaxy in VO_2 thin films due to several intrinsic problems that hamper reliable and predictable VO_2 device performance. Genuine epitaxial growth without rotational domain variants has been achieved with a TiO_2 substrate, owing to the rutile, isostructural symmet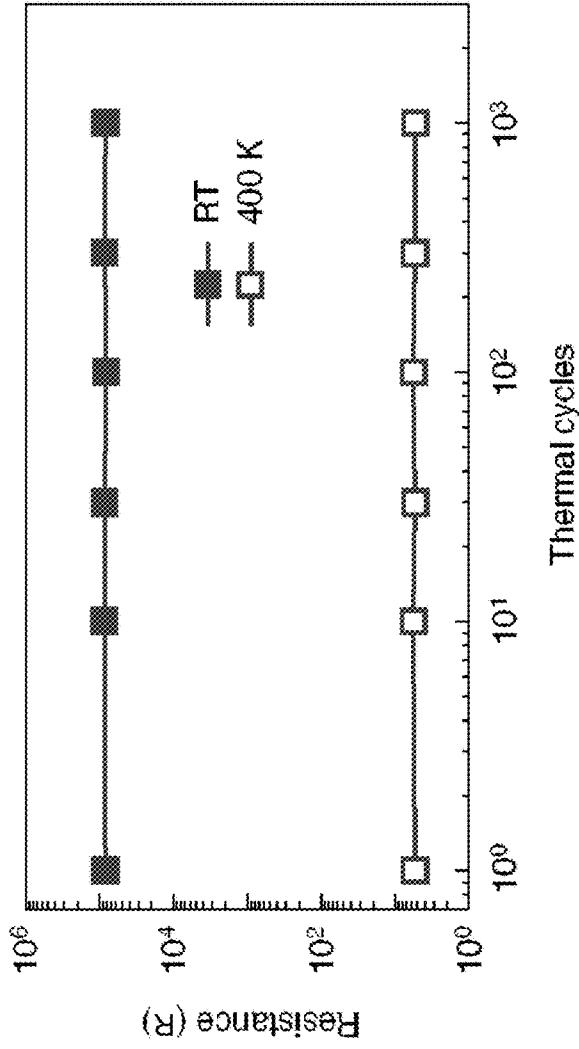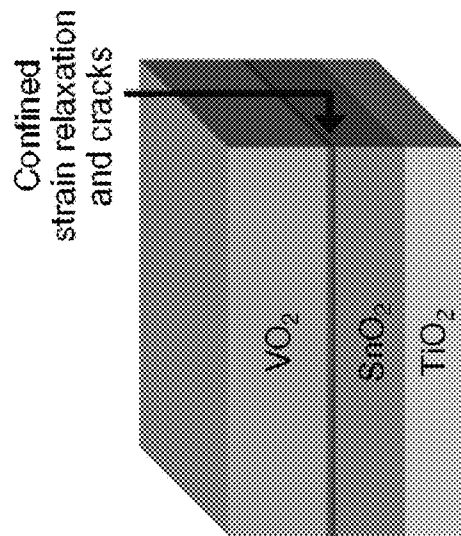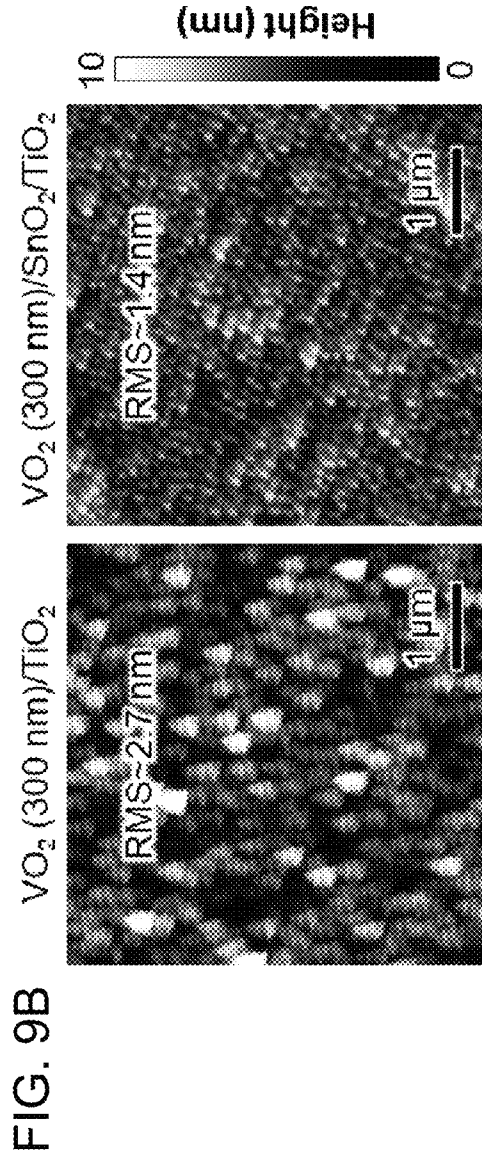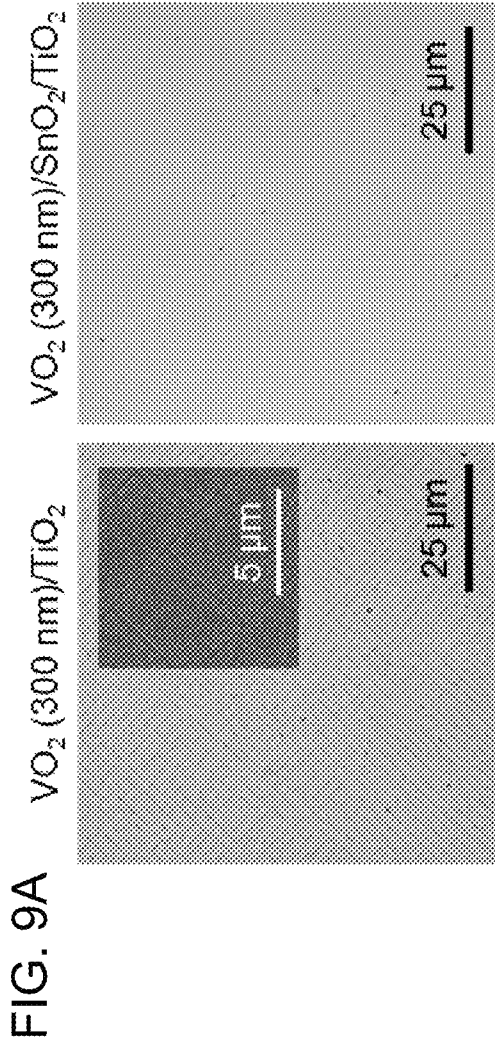ry between VO_2 and TiO_2 at their respective growth temperatures. Despite structural compatibility, though, there is a slight lattice mismatch of ~1.0% between VO_2 and TiO_2, causing a gradual strain relaxation when a film's thickness exceeds a critical value (i.e., ~20 nm), and this results in severe inhomogeneities throughout the films and in a broad MIT. Even worse, this strain relaxation is accompanied by the formation of cracks that degrade VO_2's MIT features, including its magnitude of resistance change across the MIT.

SUMMARY

Layered oxide structures comprising an overlayer of high quality VO_2 and methods of fabricating the layered oxide structures are provided. Also provided are high-speed switches comprising the layered structures and methods of operating the high-speed switches.

One embodiment of a layered oxide structure comprises: (a) a substrate comprising single-crystalline TiO_2; (b) an intervening layer comprising columnar, crystalline domains of rutile SnO_2 on the substrate, wherein the columnar, crystalline domains of SnO_2 have an epitaxial relationship with the single-crystalline TiO_2; and (c) an overlayer comprising crystalline domains of VO_2 on the intervening layer, wherein the crystalline domains of VO_2 have an epitaxial relationship with the columnar, crystalline domains of rutile SnO_2. In the structure, the VO_2 has a metal-insulator phase transition critical temperature, below which the VO_2 has a monoclinic crystal structure and above which the VO_2 has a rutile crystal structure.

One embodiment of a switch comprises: a body comprising: (a) a substrate comprising single-crystalline TiO_2; (b) an intervening layer comprising columnar, crystalline domains

of rutile SnO_2, wherein the columnar, crystalline domains of SnO_2 have an epitaxial relationship with the single-crystalline TiO_2; and (c) a channel layer comprising crystalline domains of VO_2 on the intervening layer, wherein the crystalline domains of VO_2 have an epitaxial relationship with the columnar, crystalline domains of rutile SnO_2. The VO_2 of the channel has a metal-insulator phase transition critical temperature, below which the VO_2 has a monoclinic crystal structure and above which the VO_2 has a rutile crystal structure. The switch also includes: (d) a first electrically conducting contact in electrical communication with a first area of the channel layer; (e) a second electrically conducting contact in electrical communication with a second area of the channel layer; and (f) an external stimulus source, such as an external voltage source, configured to apply a metal-insulator phase transition-inducing external stimulus to the channel layer.

One embodiment of a method for operating the switch comprises: applying an external voltage from an external voltage source to the first electrically conducting contact, wherein the external voltage induces the VO_2 to undergo a phase transition from the electrically insulating monoclinic crystal structure to the electrically conducting rutile crystal structure.

The switch can be a field effect switch comprising: a body comprising: (a) a substrate comprising single-crystalline TiO_2; (b) an intervening layer comprising columnar, crystalline domains of rutile SnO_2, wherein the columnar, crystalline domains of SnO_2 have an epitaxial relationship with the single-crystalline TiO_2; and (c) a channel layer comprising crystalline domains of VO_2 on the intervening layer, wherein the crystalline domains of VO_2 have an epitaxial relationship with the columnar, crystalline domains of rutile SnO_2. The VO_2 of the channel has a metal-insulator phase transition critical temperature, below which the VO_2 has a monoclinic crystal structure and above which the VO_2 has a rutile crystal structure. The field effect switch further includes: (d) a source; (e) a drain, wherein the source and drain are connected by the channel layer; (f) a gate stack comprising: a gate oxide on the channel layer and a gate contact on the gate oxide; and (g) an external voltage source configured to apply a metal-insulator phase transition-inducing external voltage to the gate contact.

One embodiment of a method for operating the field effect switch comprises: applying a gate voltage from the external voltage source to the gate contact, wherein the external voltage induces the VO_2 to undergo a phase transition from the electrically insulating monoclinic crystal structure to the electrically conducting rutile crystal structure.

One embodiment of a method of making a layered oxide structure comprises: epitaxially growing a layer of columnar, crystalline domains of rutile SnO_2, on a substrate comprising single-crystalline TiO_2; and epitaxially growing an overlayer comprising crystalline domains of VO_2 on the layer of columnar, crystalline domains of rutile SnO_2.

Other principal features and advantages of the invention will become apparent to those skilled in the art upon review of the following drawings, the detailed description, and the appended claims.

BRIEF DESCRIPTION OF THE DRAWINGS

Illustrative embodiments of the invention will hereafter be described with reference to the accompanying drawings, wherein like numerals denote like elements.

FIG. 1. Schematic diagram showing a multilayered structure comprising a VO_2 overlayer below its critical phase

transition temperature (right) and above its critical phase transition temperature (left). The rutile (left) and monoclinic (right) crystal structures of the VO_2 are shows above the multilayered structures.

FIG. **2**. TEM of a multilayered structure comprising a VO_2 overlayer below its critical phase transition temperature, with different rotational orientations of the VO_2 domains indicated.

FIG. **3**. Schematic diagram of a two-terminal switch with a VO_2 channel layer.

FIG. **4**. Schematic diagram of a three-terminal switch with a VO_2 channel layer.

FIG. **5A**. Atomic structures of rutile, metallic VO_2 (upper left); monoclinic, insulating VO_2 (upper right); rutile TiO_2 (lower left); and rutile SnO_2 (lower right) (corresponding lattice parameters are also shown). FIG. **5B**. Schematic diagram showing the expected lattice-strain profiles for epitaxial VO_2 films on TiO_2 without a, SnO_2 template. FIG. **5C**. Schematic diagram showing the expected lattice-strain profiles for epitaxial VO_2 films on TiO_2 with a SnO_2 template.

FIG. **6A**. Monoclinic-to-rutile structural-phase transition upon heating, modeled using in situ TEM measurements of a 300-nm-thick VO_2 film on TiO_2. The phase boundaries between monoclinic and rutile structures at each temperature are represented using solid lines. FIG. **6B**. Spatial map of out-of-plane strain ϵ_{yy} for VO_2 films on TiO_2. FIG. **6C**. Spatial map of electrical potential for VO_2 films on TiO_2. FIG. **6D**. Monoclinic-to-rutile structural-phase transition upon heating a 300-nm-thick VO_2 film on an SnO_2-templated TiO_2. FIG. **6E**. Monoclinic portion as a function of temperature T, as estimated based on the relative areas of the monoclinic regions in FIGS. **6A** and **6D**.

FIG. **7A**. Resistance R versus temperature T for the VO_2 films of the Example.

FIG. **7B**. The derivative curves of R for a 300-nm-thick VO_2 film on an SnO_2-templated TiO_2 (closed circles and squares indicate derivatives of the R logarithm, as measured during heating and cooling, respectively; experimental data are fitted using Gaussian curves [solid lines]). FIG. **7C**. Refractive index n as function of temperature and λ for the 300-nm-thick $VO_2/SnO_2/TiO_2$ film. FIG. **7D**. Extinction coefficient k as function of temperature and λ for the 300-nm-thick $VO_2/SnO_2/TiO_2$ film. FIG. **7E**. Refractive index n as function of temperature and λ for the 300-nm-thick VO_2/TiO_2 film. FIG. **7F**. Extinction coefficient k as function of temperature and λ for the 300-nm-thick VO_2/TiO_2 film.

FIG. **8A**. Schematic drawing showing strain relaxation and cracking in VO_2 films without SnO_2 templates; in the VO_2 film on an SnO_2-templated TiO_2, severe structural defects, such as strain relaxation and cracks, were well-confined to the interface, and this protects such films against degradation caused by repeated phase transitions. FIG. **8B**. Resistance, measured at room temperature and 400 K, after repeated phase transitions of the VO_2 films without SnO_2 templates. FIG. **8C**. Schematic drawing showing strain relaxation and cracking in VO_2 films with SnO_2 templates; in the VO_2 film on an SnO_2-templated TiO_2, severe structural defects, such as strain relaxation and cracks, were well-confined to the interface, and this protects such films against degradation caused by repeated phase transitions. FIG. **8D**. Resistance, measured at room temperature and 400 K, after repeated phase transitions of the VO_2 films with SnO_2 templates.

FIG. **9A**. Microscopic images of the VO_2 films' surfaces for VO_2 grown on TiO_2 (left) and on SnO_2/TiO_2 (right); the

image in the inset shows a film surface as observed with a scanning electron microscopy (SEM); prior to SEM imaging, the film surface was chemically etched to observe the resultant cracks more clearly. FIG. **9B**. AFM images of the VO_2 films' surfaces for VO_2 grown on TiO_2 (left) and SnO_2/TiO_2 (right).

DETAILED DESCRIPTION

Layered oxide structures comprising an overlayer of high quality VO_2 and methods of fabricating the layered oxide structures are provided. Also provided are high-speed switches comprising the layered structures and methods of operating the high-speed switches.

The layered oxide structures comprise high quality VO_2 epitaxial films grown on a symmetrically isostructural SnO_2 template. The lattice mismatch between the VO_2 and SnO_2 produces small, well-connected domains of VO_2 having the same crystal structure in the epitaxial film and confines severe structural defects (e.g., strain gradients and cracks) to the area near the SnO_2/VO_2 interface. This leads to homogeneous, bulk-like lattices in the VO_2 film, without compromising the film's epitaxial nature. This structural homogeneity also enables homogeneous electronic and chemical states throughout the films, which is highly desirable for creating reliable, high performance devices, such as high-speed switches.

The VO_2 in the epitaxial films is characterized by a metal-insulator phase transition critical temperature. Below this critical temperature, the VO_2 in the epitaxial crystalline domains has an electrically insulating monoclinic crystal structure. As the VO_2 is heated to and above its critical temperature, the crystal structure transitions to a metallic conducting rutile crystal structure. In the VO_2 films, the transition is very sharp and is accompanied by a large decrease in the films' electrical resistance. In addition, the small crystalline domains in the VO_2 films help them to absorb the stresses and strains that accompany the phase transition, enabling the films to undergo many phase transition cycles without cracking. As a result, the VO_2 films are well suited for switching applications. For example, the VO_2 films can be used in electronic switches and optoelectronic switches in circuits, including integrated circuits, for memory devices (e.g., CMOS chips) and communication devices.

One embodiment of a layered structure comprising a VO_2 overlayer is shown schematically in FIG. **1**. The right side the figure shows the structure at a first temperature that is below the phase transition critical temperature (T_{crit}) and the left side of the figure shows the structure at a second temperature that is above the T_{crit}. The structure comprises a single-crystalline, rutile TiO_2 substrate **102** having an exposed TiO_2 (001) growth surface. A template layer **106** comprising columnar crystalline domains of rutile SnO_2 is disposed on TiO_2 substrate **102**. The columnar, crystalline domains of rutile SnO_2 are grown epitaxially and, therefore, have an epitaxially relationship with the underlying TiO_2. Rutile SnO_2 domains have an exposed (001) surface on which an overlayer **110** comprising a plurality of connected crystalline VO_2 domains of is disposed. Epitaxial growth of the SnO_2 and VO_2 can be accomplished using, for example, pulsed laser deposition (PLD) as illustrated in the Example.

The lattice mismatch between the TiO_2 substrate and the SnO_2 results in the epitaxial, nanoscale, crystalline columnar domains in the SnO_2 growing upward from the TiO_2 growth surface. These domains, which have the same crystal structure (rutile) and orientation nucleate separately on the

growth surface and grow together to a growth template that is isostructural with the subsequently grown VO_2 at growth temperatures above T_{crit}. As such, the SnO_2 films are not polycrystalline films in which a plurality of crystal domains are oriented randomly within the film. As used herein, the term nanoscale columnar domains refers to columnar domains having average cross-sectional diameters that are no greater than 200 nm. This includes columnar domains having average cross-sectional diameters that are no greater than 100 nm; no greater than 50 nm; and no greater than 20 nm. For example, in some embodiments of the SnO_2 films, the columnar domains have average cross-sectional diameters in the range from about 5 nm to about 10 nm. The thickness of the SnO_2 layer is typically in the range from about 100 nm to about 300 nm, but thicknesses outside of this range can be used.

The lattice mismatch between the SnO_2 and the VO_2 limits the size of the epitaxially grown VO_2 domains and concentrates and/or confines any cracks in the VO_2 film to a small volume near the SnO_2/VO_2 interface, while the remainder of the VO_2 may be crack- and strain-free. This is advantageous because it allows the VO_2 layers to be grown to commercially practical thicknesses without any significant cracking beyond the lowermost portion of the layer. By way of illustration only, in some embodiments of the layered structures, the VO_2 layer has a thickness of at least 100 nm. This includes layered structures having a VO_2 layer thicknesses of at least 200 nm and further includes layered structures having a VO_2 layer thicknesses of at least 300 nm. For example, in some embodiments, the VO_2 layer thickness is in the range from about 100 nm to about 500 nm. This includes embodiments in which the VO_2 layer thickness is in the range from about 200 nm to about 400 nm. In each of these embodiments, the cracks and/or strains (if present at all) may be confined to within a few nanometers (for example, 10 nm or fewer, including 5 nm or fewer) of the SnO_2/VO_2 interface.

The small size of the VO_2 domains helps the VO_2 film to absorb the stresses and strains of the MIT, which reduces cracking during phase change cycling and improves and sustains device performance. As used here, the size of the domains refers to the largest cross-sectional width of the domains, where the width dimension is perpendicular to the thickness dimension. In some embodiments of the layered structures, the average width of the VO_2 domains is no greater than about 500 nm. This includes embodiments in which the average width of the VO_2 domains is no greater than about 400 nm and further includes embodiments in which the average width of the VO_2 domains is no greater than about 300 nm. The VO_2 domains are well-connected, have a common crystal structure and an epitaxial relationship with the underlying SnO_2. At temperatures below T_{crit}, the VO_2 has a monoclinic crystal structure and is electrically insulating. The monoclinic VO_2 domains can have four different rotational orientations that are rotated by 90° from each other in the plane of the film. The different rotations domains are represented by area of different shading in overlayer **110** on the right side of FIG. **1**. The four different rotational domain variants of the monoclinic VO_2 are shown in the upper right side of FIG. **1**. At temperatures above T_{crit}, the VO_2 has a tetragonal rutile crystal structure and acts as an electrical conductor. The rutile crystal structure is shown in the upper left side of FIG. **1**.

The T_{crit} for the VO_2 in the overlayer is greater than room temperature (i.e., greater than 300 K). Typically, the T_{crit} is greater than 340 and in the range from about 338 to about 345 K (e.g., about 340 to 343 K, including about 341 K).

(Unless otherwise indicated, the phase transition critical temperatures referred to in this disclosure refer to the critical temperature in the absence of an applied external field or strain.)

The high quality VO_2 films grown on SnO_2 template layers can be characterized by their sharp metal-insulator phase transitions, where the sharpness of a transition is characterized by the full width at half maximum (FWHM) of the derivative curve of a heating curve, as illustrated in the Example. Some embodiments of the VO_2 films have a phase transition sharpness of 2 K or less. This includes VO_2 films having a phase transition sharpness of 1.5 K or less and further includes VO_2 films having a phase transition sharpness of 1 K or less. These sharp transition can be achieved even in films with thicknesses above 100 nm, above 200 nm, and above 300 nm.

The monoclinic to rutile (insulating to conducting) phase transition is accompanied by a large drop in the vanadium dioxide's magnitude of electrical resistance (ΔR), which can be measured as described in the Example. Some embodiments of the VO_2 films have a ΔR of at least 2 orders of magnitude. This includes VO_2 films having a ΔR of at least 3 orders of magnitude and further includes VO_2 films having a ΔR of at least 4 orders of magnitude.

The layered structure can be used as a switch by heating the VO_2 above its T_{crit} to trigger the phase transition. Devices configured to induce or monitor this heating-induced switching can be used as thermal switches and thermal sensors. Alternatively, an external stimulus, such as an electric field, an optical field, a mechanical strain, or a combination thereof, can be applied to the VO_2 to induce the phase transition. These external stimuli shift the critical temperature for the MIT and induce the reversible phase transition, which changes the resistance (and, therefore, conductance) of the VO_2, thereby modulating current flow through the material. Devices configured for field-induced switching can be used as high-speed switches for a variety of electronic, optical, and optoelectronic applications. A basic embodiment of a two-terminal switch comprising the layered structure is shown in the schematic diagram of FIG. **3**. This switch is designed to undergo an electric field-induced crystalline phase transition. The switch comprises a channel layer comprising the crystalline domains of VO_2 **302**, a first electrically conducting contact **304** in electrical communication with layer **302**, and a second electrically conducting contact **306** in electrical communication with layer **302**. The switch embodiment shown here also includes a dielectric substrate **307** comprising the SnO_2 **308** and TiO_2 **309** layers of the layered structure. The crystalline phase change in the VO_2 channel layer can be triggered by the application of an external electric field. This is typically accomplished by applying an external voltage from an external voltage source to first electrically conducting contact **304**. If the magnitude of the applied voltage is meets a certain voltage threshold, it will induce the phase change and trigger the switch.

FIG. **4** is a schematic diagram of the three-terminal field effect switch that incorporates a VO_2 layer as a channel. The switch comprises a source **412**, a drain **414**, and a channel layer comprising the crystalline domains of VO_2 **402** disposed between source **412** and drain **414**. A gate stack comprising a gate dielectric **416** and a gate contact **418** is disposed on channel layer **402**. The field effect switch also includes a dielectric substrate **407** comprising the SnO_2 **408** and TiO_2 **409** layers of the layered structure. The crystalline phase change in the VO_2 channel layer can be triggered by the application of a gate voltage, such as a negative gate

voltage, to gate contact **418**. If the applied gate voltage is greater than the threshold voltage, it will induce the phase change and trigger the switch.

Although the switches shown in FIGS. **3** and **4** include the SnO_2 template layer and TiO_2 substrate upon which the VO_2 layer is grown, it is also possible to remove one or both of these layers after VO_2 layer growth and then transfer the VO_2 layer onto another support substrate, which may be an electrically conducting (metallic), semiconducting, or electrically insulating substrate.

EXAMPLE

In this example, VO_2 films were grown on an SnO_2-templated TiO_2 (001) substrate. SnO_2 is insulating and has a rutile symmetry isostructural with VO_2 at its growth temperature, making it relevant as a template for epitaxial VO_2 growth (FIG. **5A**). A large lattice mismatch ($\geq 4.2\%$) between VO_2 and SnO_2 results in an abrupt strain relaxation at the interface region within a few nanometers. As a result, severe structural defects, including strain gradient, were confined only near the interface between the VO_2 and SnO_2, leading to homogeneous, bulk-like lattices in the VO_2 film (FIG. **5C**) and a sharp MIT above room temperature. Additionally, the low solid solubility between VO_2 and SnO_2 significantly enhanced the materials' chemical sharpness at the interface by reducing interfacial intermixing. Thus, thin-film epitaxy using an SnO_2 template is a suitable process for producing homogeneous, crystalline, crack-free VO_2 films.

Materials and Methods

Crystalline VO_2 epitaxial thin films were grown on (001) TiO_2 substrates using the pulsed laser deposition (PLD) method. Before deposition, low miscut 0.1°) TiO_2 substrates were cleaned by sonicating with acetone and then rinsing with isopropanol. An SnO_2 epitaxial layer with a thickness of 100 nm was deposited as a bottom template on the TiO_2 substrate. A KrF excimer laser ($\lambda=248$ nm) beam was focused on SnO_2 and V_2O_5 ceramic targets to an energy density of ~2.0 J/cm^2 and pulsed at 5 Hz (for SnO_2 layer) or 10 Hz (for VO_2 layer). SnO_2 layers were grown at a substrate temperature of 400° C. and oxygen partial pressure of 50 mTorr. After growth of the SnO_2 layer, the VO_2 layer was grown at the temperature of 400° C. and oxygen partial pressure of 18 mTorr. After growth, the VO_2/SnO_2 films were cooled down to room temperature at an oxygen partial pressure of 18 mTorr.

The structural qualities of the films were examined using high-resolution X-ray diffraction (XRD). The XRD pattern of the $VO_2/SnO_2/TiO_2$ film showed a clear film peak at $2\theta=64.8°$ along with (002) diffraction peaks from the underlying rutile SnO_2 and TiO_2 substrate. This film peak comes from the ($\overline{4}02$) reflection of monoclinic VO_2, and these correspond with the (002) reflection of VO_2's high-temperature rutile phase. No other peaks were observed using XRD analysis, proving that the VO_2 film was highly oriented and had a pure phase. The peak position (i.e., $2\theta=64.7°$) was almost identical to that of the ($\overline{4}02$) reflection for bulk, monoclinic VO_2, suggesting that the film was fully relaxed and had bulk-like lattices. Importantly, the $VO_2/SnO_2/TiO_2$ film exhibited a symmetric diffraction peak, well fitted with a single peak, implying that the misfit strain was abruptly relaxed without gradual strain relaxation. In contrast, the VO_2/TiO_2 film exhibited an asymmetrical diffraction peak, implying the presence of a gradual strain relaxation in the film, consistent with this study's initial predictions.

To obtain further information on lattice strains, X-ray reciprocal-space mappings (RSMs) were used. In the case of

the VO_2/TiO_2 film, the film's RSM peak position (denoted by a closed, circle) was far from that of the VO_2's bulk (denoted by a closed, star), indicating that the VO_2 film was still partially strained. Furthermore, the film's RSM peak featured a shoulder directed toward the bulk peak position, confirming gradual strain relaxation in the film. As for the $VO_2/SnO_2/TiO_2$ film, the peak position of the film was identical to that of the bulk VO_2. This indicates that the use of an SnO_2 template leads to homogeneous lattices, as well as to complete relaxation for the misfit strain in the VO_2 film.

Results

Based on initial predictions, structural inhomogeneity determined the MIT behavior of the VO_2 films. To visualize the role of local inhomogeneities on MIT, in situ transmission electron microscopy (TEM) was used. The monoclinic-to-rutile structural phase transition was monitored by heating the VO_2 films. Abrupt changes to lattice parameters (FIG. **5A**), as well as to symmetry, during the phase transition caused noticeable contrast between the monoclinic and rutile regions, allowing clear visualization of the structural phase transition. For VO_2 films on bare TiO_2, the rutile phase started to nucleate from the interface at ~315 K, which is much lower than the nucleation point for bulk T_{MIT} (i.e., 341 K), and the phase transition was complete near the surface and cracks. The local profile of the films' respective strains and electric potentials were measured using inline holography (FIGS. **6B**, **6C**), and there was a close relationship between local strain and T_{MIT}. However, whereas regions near the surface and cracks experienced negligible strain in the bulk-like T_{MIT}, the interfacial regions with relatively more strain preferred the rutile structure and had much lower T_{MIT}, resulting in a broad MIT (FIG. **6E**).

In contrast, the VO_2 film on SnO_2-templated TiO_2 exhibited a much sharper, bulk-like phase transition and did not exhibit any structural or electronic inhomogeneities distinct from those of the VO_2 film on bare TiO_2. As a result, the VO_2 film on SnO_2/TiO_2 had a much sharper transition, and most of its structural-phase transition was complete between 341 and 343 K (FIGS. **6D**, **6E**). Interestingly, for the VO_2 film on SnO_2/TiO_2, the structural phase transition began at the surface and ended at the interface, which is the opposite of how the transition progresses in VO_2 films on bare TiO_2 (FIG. **6A**). These phase-field simulations reveal that homogeneous VO_2 single crystals have a monoclinic-to-rutile phase transition that begins at the surface. Thus, the present study's in situ TEM and simulation results demonstrate that placing a VO_2 epitaxial film on an SnO_2-templated TiO_2 offers a more reliable, enhanced MIT, whose sharpness and magnitude are as good as those of intrinsic VO_2 single crystals.

To characterize the MIT and its sharpness, electrical resistance was measured as a function of temperature in VO_2 films with or without an SnO_2 template (FIG. **7A**). The resistance of the 300-nm-thick VO_2 film on the SnO_2/TiO_2 substrate caused a change of four orders of magnitude (i.e., $\geq 3 \times 10^6\%$) during MIT, while the resistance change was drastically reduced in VO_2 films on bare TiO_2, possibly due to the presence of a strain gradient and cracks (FIGS. **9A** and **9B**). The transition temperature for the $VO_2/SnO_2/TiO_2$ film was ~341 K, the same as for the bulk VO_2. As FIG. **7A** also clearly shows, the $VO_2/SnO_2/TiO_2$ film exhibited a much sharper MIT compared with films of the same thickness on bare TiO_2. The sharpness of the $VO_2/SnO_2/TiO_2$ film's MIT was quantitatively estimated to be <1 K using the width of its derivative curves (FIG. **7B**). This MIT sharpness (i.e., ~0.5 K) is comparable to that of fully coherent, 10-nm-thick VO_2 films on bare TiO_2. Thus, this study's electrical-trans-

port measurements indicate that homogeneity engineering using an SnO_2 template allows for a sharp, pronounced resistance change across MIT, while maintaining a bulk-like transition temperature.

Thus far, electrical-transport measurements have been used to determine the sharpness of the MIT. However, electrical conduction can be dominated by low-resistive local regions and associated short-circuit currents so that the transport measurements might not effectively reflect MIT sharpness for the overall film region. Because of this, optical measurements were adopted in addition to electrical measurements. Using spectroscopic ellipsometry, refractive index n and extinction coefficient k were measured as a function of temperature. It is known that the complex dielectric function and associated n and k exhibit a noticeable change during MIT. (See, J. B. Kana Kana et al., Opt. Commun. 284, 807 (2011).) Furthermore, in contrast to electrical measurements, measurements of n and k are governed by the averaged optical response for the whole film region, rather than for local regions alone. Thus, optical measurements of n and k effectively reveal genuine MIT features, such as sharpness, in VO_2 films.

FIGS. 7C-F show the values for n and k measured during heating as functions of temperature, as well as wavelength A of incidental light for 300-nm-thick VO_2 films. For the $VO_2/SnO_2/TiO_2$ film (FIGS. 3C, 3D), n and k exhibited abrupt changes for every λ across MIT with a T_{MIT} of ~341 K, and this was the same as with the bulk sample. This sharp transition in n and k is attributable to the film's homogeneous nature (FIG. 5C). And yet, for the VO_2/TiO_2 film (FIGS. 7E, 7F), n and k exhibited gradual changes across MIT with an average T_{MIT} of ~320 K, and this is attributable to the film's local inhomogeneities (FIG. 5B). Furthermore, the lower average T_{MIT} value compared with the bulk value is attributable to the film's average tensile strain. Thus, these optical measurements confirm that the $VO_2/SnO_2/TiO_2$ film had a sharp MIT, and they underscore the importance of homogeneity engineering in producing high-quality epitaxial VO_2 films.

Last, SnO_2 template's contributions were examined to prevent the VO_2 from cracking. VO_2 bulk crystals tend to crack under large amounts of stress during MIT, and they degrade upon repeat cycling. Strain relaxation in VO_2 epitaxial films can also cause such cracks (FIG. 8A). In this study, an increasing number of such cracks were formed after repeated thermal cycles, and they severely affected the MIT features of the VO_2 film on bare TiO_2. A more significant, increased resistance to cracks occurred during the nominally metallic phase, and as a result, the magnitude of resistance change across the MIT was far less, down to ~$10^5\%$. On the other hand, the VO_2 films on SnO_2/TiO_2 had robust MITs, and the magnitude of their resistance change remained at ~$10^6\%$, even after 1,000 cycles. This indicates that, once confined to the interface, structural defects like cracks don't spread into the films after repeated cycles with $VO_2/SnO_2/TiO_2$ films.

This example demonstrates thin-film epitaxy of structurally homogeneous, crack-free VO_2 with a sharp, reliable MIT grown using an SnO_2 template layer. Furthermore, correlated electron materials have exhibited various other novel phenomena in addition to the MIT, including superconductivity and colossal magnetoresistance—both of which are desirable for emerging electronics applications. These properties are, generally, strongly dependent on lattice strain due to a combination of charge, spin, orbitals, and degrees of lattice freedom. Thus, this study provides a general framework for predictively designing homogenous,

heteroepitaxial materials with reliable electronic functions that include, but are not limited to, material MIT.

The word "illustrative" is used herein to mean serving as an example, instance, or illustration. Any aspect or design described herein as "illustrative" is not necessarily to be construed as preferred or advantageous over other aspects or designs. Further, for the purposes of this disclosure and unless otherwise specified, "a" or "an" means "one or more".

The foregoing description of illustrative embodiments of the invention has been presented for purposes of illustration and of description. It is not intended to be exhaustive or to limit the invention to the precise form disclosed, and modifications and variations are possible in light of the above teachings or may be acquired from practice of the invention. The embodiments were chosen and described in order to explain the principles of the invention and as practical applications of the invention to enable one skilled in the art to utilize the invention in various embodiments and with various modifications as suited to the particular use contemplated. It is intended that the scope of the invention be defined by the claims appended hereto and their equivalents.

What is claimed is:

1. A layered oxide structure comprising:
a substrate comprising single-crystalline TiO_2;
an intervening layer comprising columnar, crystalline domains of rutile SnO_2 on the substrate, wherein the columnar, crystalline domains of SnO_2 have an epitaxial relationship with the single-crystalline TiO_2; and
an overlayer comprising crystalline domains of VO_2 on the intervening layer, wherein the crystalline domains of VO_2 have an epitaxial relationship with the columnar, crystalline domains of rutile SnO_2;
wherein the VO_2 has a metal-insulator phase transition critical temperature, below which the VO_2 has a monoclinic crystal structure and above which the VO_2 has a rutile crystal structure.

2. The structure of claim 1, wherein the metal-insulator phase transition critical temperature is in the range from 339 to 343 K.

3. The structure of claim 1, characterized in that, when the overlayer is heated from a temperature below its metal-insulator phase transition critical temperature to a temperature above its metal-insulator phase transition critical temperature, the VO_2 undergoes a phase transition from monoclinic to rutile with a transition sharpness of no greater than 2 K.

4. The structure of claim 3, characterized in that, when the overlayer is heated from a temperature below its metal-insulator phase transition critical temperature to a temperature above its metal-insulator phase transition critical temperature, the VO_2 undergoes a phase transition from monoclinic to rutile and the electrical resistance of the overlayer decreases by at least four orders of magnitude.

5. The structure of claim 1, characterized in that, when the overlayer is heated from a temperature below its metal-insulator phase transition critical temperature to a temperature above its metal-insulator phase transition critical temperature, the VO_2 undergoes a phase transition from monoclinic to rutile with a transition sharpness of no greater than 1 K.

6. The structure of claim 5, characterized in that, when the overlayer is heated from a temperature below its metal-insulator phase transition critical temperature to a temperature above its metal-insulator phase transition critical temperature, the VO_2 undergoes a phase transition from

monoclinic to rutile and the electrical resistance of the overlayer decreases by at least four orders of magnitude.

7. The structure of claim 1, characterized in that, when the overlayer is heated from a temperature below its metal-insulator phase transition critical temperature to a temperature above its metal-insulator phase transition critical temperature, the VO_2 undergoes a phase transition from monoclinic to rutile and the electrical resistance of the overlayer decreases by at least four orders of magnitude.

8. The structure of claim 1, wherein the overlayer has a thickness in the range from 100 to 500 nm.

9. The structure of claim 8, wherein the overlayer has a thickness in the range from 200 to 400 nm.

10. A switch comprising:
a body comprising: a substrate comprising single-crystalline TiO_2; an intervening layer comprising columnar, crystalline domains of rutile SnO_2, wherein the columnar, crystalline domains of SnO_2 have an epitaxial relationship with the single-crystalline TiO_2; and a channel layer comprising crystalline domains of VO_2 on the intervening layer, wherein the crystalline domains of VO_2 have an epitaxial relationship with the columnar, crystalline domains of rutile SnO_2, and further wherein the VO_2 has a metal-insulator phase transition critical temperature, below which the VO_2 has a monoclinic crystal structure and above which the VO_2 has a rutile crystal structure;
a first electrically conducting contact in electrical communication with a first area of the channel layer;
a second electrically conducting contact in electrical communication with a second area of the channel layer; and
an external stimulus source configured to apply a metal-insulator phase transition-inducing external stimulus to the channel layer.

11. The switch of claim 10, wherein the external stimulus source configured to apply a metal-insulator phase transition-inducing external stimulus to the channel layer is an external voltage source configured to apply an external voltage to the first electrically conducting contact.

12. A method of switching using the switch of claim 11, the method comprising applying an external voltage from the external voltage source to the first electrically conduct-ing contact, wherein the external voltage induces the VO_2 to undergo a phase transition from the electrically insulating monoclinic crystal structure to the electrically conducting rutile crystal structure.

13. A field effect switch comprising:
a body comprising: a substrate comprising single-crystalline TiO_2; an intervening layer comprising columnar, crystalline domains of rutile SnO_2, wherein the columnar, crystalline domains of SnO_2 have an epitaxial relationship with the single-crystalline TiO_2; and a channel layer comprising crystalline domains of VO_2 on the intervening layer, wherein the crystalline domains of VO_2 have an epitaxial relationship with the columnar, crystalline domains of rutile SnO_2, and further wherein the VO_2 has a metal-insulator phase transition critical temperature, below which the VO_2 has a monoclinic crystal structure and above which the VO_2 has a rutile crystal structure;
a source;
a drain, wherein the source and drain are connected by the channel layer;
a gate stack comprising: a gate oxide on the channel and a gate contact on the gate oxide; and
an external voltage source configured to apply a metal-insulator phase transition-inducing external voltage to the gate contact.

14. A method of switching using the switch of claim 13, the method comprising:
applying a gate voltage from the external voltage source to the gate contact, wherein the external voltage induces the VO_2 to undergo a phase transition from the electrically insulating monoclinic crystal structure to the electrically conducting rutile crystal structure.

15. A method of making a layered oxide structure, the method comprising:
epitaxially growing a layer of columnar, crystalline domains of rutile SnO_2, on a substrate comprising single-crystalline TiO_2; and
epitaxially growing an overlayer comprising crystalline domains of VO_2 on the layer of columnar, crystalline domains of rutile SnO_2.

*   *   *   *   *